Analysis of mirror soft-x-ray–EUV scattering using generalized continuous growth model of multiscale reliefs

Leonid Goray[1,2] and Maxim Lubov[1,3,*]

[1]*Saint Petersburg Academic University, 8/3 L."A", Khlopin str., St. Petersburg 194021, Russia*
[2]*Institute for Analytical Instrumentation, 31-33 L."A", Ivana Chernykh str., St. Petersburg 198095, Russia*
[3]*Ioffe Institute, 26, Politekhnicheskaya str., St. Petersburg 194021, Russia*
[*]*lubov@spbau.ru*

Abstract: Combined computer simulations of the growth of multilayer mirrors and their exact differential reflection coefficients in the soft-x-ray–EUV range have been conducted. The proposed model describes the variation of the surface roughness of the multilayer Al/Zr mirror boundary profiles taking into account a random noise source. Theoretically calculated Al/Zr boundary profiles allow one to know real rough boundary statistics including rms roughnesses and correlation lengths and, to obtain rigorously EUV specular and diffuse reflection coefficients. The proposed integrated approach opens up a way to performing exact theoretical studies similar in accuracy to results obtained by quantitative microscopy investigations of nanoreliefs and synchrotron radiation measurements.

OCIS codes: (310.6805) Theory and design; (290.5880) Scattering, rough surfaces; (050.1755) Computational electromagnetic methods; (340.7470) X-ray mirrors.

References and links

1. V. E. Asadchikov, I. V. Kozhevnikov, Yu. S. Krivonosov, R. Mercier, T. H. Metzger, C. Morawe, and E. Ziegler, "Application of X-ray scattering technique to the study of supersmooth surfaces," Nucl. Inst. Meth. Phys. Res. A. **530**, 575–595 (2004).
2. L. Goray and M. Lubov, "Nonlinear continuum growth model of multiscale reliefs as applied to rigorous analysis of multilayer short-wave scattering intensity. I. Gratings," J. Appl. Cryst. **46**(4), 926–932 (2013).
3. U. Pietsch, V. Holy, and T. Baumbach, *High-Resolution X-Ray Scattering: From Thin Films to Lateral Nanostructure*, (Springer-Verlag, 2004).
4. L. I. Goray, I. G. Kuznetsov, S. Yu. Sadov, and D. A. Content, "Multilayer resonant subwavelength gratings: effects of waveguide modes and real groove profiles," J. Opt. Soc. Am. A **23**(1), 155–165 (2006).
5. L. I. Goray, "Solution of the inverse problem of diffraction from low-dimensional periodically arranged nanocrystals," Proc. SPIE **8083**, 80830L (2011).
6. I. Kozhevnikov, L. Peverini, and E. Ziegler, "Exact determination of the phase in time-resolved X-ray reflectometry," Opt. Express **16**(1), 144–149 (2008).
7. M.-A. Henn, H. Gross, F. Scholze, M. Wurm, C. Elster, and M. Bär, "A maximum likelihood approach to the inverse problem of scatterometry," Opt. Express **20**(12), 12771–12786 (2012).
8. L. I. Goray, "Application of the rigorous method to x-ray and neutron beam scattering on rough surfaces," J. Appl. Phys. **108**(3), 033516 (2010).
9. L. I. Goray and G. Schmidt, "Boundary Integral Equation Methods for Conical Diffraction and Short Waves," in *Gratings: Theory and Numerical Applications*, E. Popov, ed. (Presses universitaires de Provence, Sec. rev. ed., 2014).
10. M. Pelliccione and L. Toh-Ming, *Evolution of Thin Film Morphology: Modeling and Simulations* (Springer, 2008).
11. W. W. Mullins, "Theory of thermal grooving," J. Appl. Phys. **28**(3), 333–339 (1957).
12. L. Goray and M. Lubov, "Nonlinear continual growth model of nonuniformly scaled reliefs as applied to the rigorous analysis of the X-ray scattering intensity of multilayer mirrors and gratings," J. Surf. Investig. X-Ra. **8**(3), 444–455 (2014).
13. D. G. Stearns, D. P. Gaines, D. W. Sweeney, and E. M. Gullikson, "Nonspecular x-ray scattering in a multilayer-coated imaging system," J. Appl. Phys. **84**(2), 1003–1028 (1998).
14. L. Peverini, E. Ziegler, and I. Kozhevnikov, "Dynamic scaling in ion etching of tungsten films," Appl. Phys. Lett. **91**(5), 053121 (2007).

#232880 - $15.00 USD Received 20 Jan 2015; revised 20 Mar 2015; accepted 22 Mar 2015; published 16 Apr 2015

15. D. L. Voronov, E. H. Anderson, R. Cambie, E. M. Gullikson, F. Salmassi, T. Warwick, V. V. Yashchuk, and H. A. Padmore, "Roughening and smoothing behavior of Al/Zr multilayers grown on flat and saw-tooth substrates," Proc. SPIE **8139**, 81390B (2011).
16. Y. V. Yashchuk and V. V. Yashchuk, Q. Zhong, "Reliable before-fabrication forecasting of expected surface slope distributions for x-ray optics," Opt. Eng. **51**(4), 046501 (2012).
17. V. V. Yashchuk, Y. N. Tyurin, and A. Y. Tyurina, "Application of the time-invariant linear filter approximation to parametrization of surface metrology with high-quality x-ray optics," Opt. Eng. **53**(8), 084102 (2014).
18. E. L. Church, P. Z. Takacs, and T. A. Leonard, "The prediction of BRDFs from surface profile measurements," Proc. SPIE **1165**, 136–150 (1990).
19. G. Rasigni, F. Varnier, M. Rasigni, J. P. Palmari, and A. Llebaria, "Roughness spectrum and surface plasmons for surfaces of silver, copper, gold, and magnesium deposits," Phys. Rev. B **27**(2), 819–830 (1983).
20. E. L. Church, "Fractal surface finish," Appl. Opt. **27**(8), 1518–1526 (1988).
21. Q. Zhong, Z. Zhang, S. Ma, R. Qi, J. Li, Z. Wang, K. Le Guen, J.-M. André, and P. Jonnard, "The transition from amorphous to crystalline in Al/Zr multilayers," J. Appl. Phys. **113**(13), 133508 (2013).
22. D. L. Voronov, E. H. Anderson, R. Cambie, S. Cabrini, S. D. Dhuey, L. I. Goray, E. M. Gullikson, F. Salmassi, T. Warwick, V. V. Yashchuk, and H. A. Padmore, "A 10,000 groove/mm multilayer coated grating for EUV spectroscopy," Opt. Express **19**(7), 6320–6325 (2011).
23. A. A. Maradudin, ed., *Light Scattering and Nanoscale Surface Roughness* (Springer, 2007).
24. L. I. Goray, "Specular and diffuse scattering from random asperities of any profile using the rigorous method for x-rays and neutrons," Proc. SPIE **7390**, 73900V (2009).
25. The Center for X-Ray Optics, X-ray Interactions With Matter, available from: *http://henke.lbl.gov/optical_constants/*.
26. E. D. Palik, ed., *Handbook of Optical Constant of Solids* (Academic, 1985).
27. J. F. Seely, L. Goray, D. L. Windt, B. Kjornrattanawanich, Y. Uspenskii, and A. V. Vinogradov, "Extreme ultraviolet optical constants for the design and fabrication of multilayer gratings," Proc. SPIE **5538**, 43–52 (2004).
28. K. Le Guen, M.-H. Hu, J.-M. André, P. Jonnard, S. K. Zhou, H. C. Li, J. T. Zhu, Z. S. Wang, N. Mahne, A. Giglia, and S. Nannarone, "Introduction of Zr in nanometric periodic Mg/Co multilayers," Appl. Phys., A Mater. Sci. Process. **102**(1), 69–77 (2011).
29. Web site, *http://www.pcgrate.com/*.

1. Introduction

Advances in fabrication of multilayer x-ray optics of the diffraction quality with subatomic roughness are primarily driven by progress in vacuum techniques and chemistry of materials, as well as by considerable achievements in Si microelectronics. In spite of the huge success, extension of the relevant research is essential due to urgent demands for the development of novel and improvement of existing optical and electronic instrumentation in such areas as beyond extreme ultraviolet (BEUV) lithography, x-ray free-electron lasers, resonant inelastic x-ray scattering, soft x-ray and EUV astrophysics, soft x-ray microscopy and various components of nano- optoelectronics. As a consequence of this the quality of multilayer boundary profiles is very important since it influences the optical properties of instruments, and therefore necessitates the accurate characterization.

The exact boundary profiles of multilayers can be derived by the few ways, to wit, extracted from the measurements, generated with defined statistical parameters and determined from the film growth simulation. In experimental characterization of the evolution of thin-film boundary profiles one widely accepts microscopic methods, such as transmission electron microscopy (TEM), atomic force microscopy (AFM) and near-field scanning optical microscopy (NSOM). Besides the fact that microscopic methods allows just to study local characteristics of the structure formed, TEM is destructive, while AFM and NSOM determine only surface boundary profiles. Also NSOM has a non-atomic scale resolution. For exactly known and rather simple boundary profile statistics, profiles themselves can be generated by various methods, see, e.g., references in [1].

One of the modern and universal approaches to investigation of the layer morphology and composition is a combination of short-wave (from hard x-rays to EUV) reflectometry or scatterometry and thin-film growth models [2]. Reflectometry permits one to determine with a high precision and in an integral way the characteristics of multilayers [3, 4], however exact theoretical and numerical approaches are needed for the solution of poorly and ambiguously solvable direct and inverse problems in reflectometry [5–7]. In this study we employ a novel powerful approach (modified method of boundary integral equations (MIM)) [8, 9] to analysis of the effect of mirror boundary profiles with complicated rough interfaces on the

#232880 - $15.00 USD Received 20 Jan 2015; revised 20 Mar 2015; accepted 22 Mar 2015; published 16 Apr 2015

soft-x-ray–EUV scattering intensity. Similarly, purely theoretical methods together with computer simulations can be used effectively for description of the process of formation of surface reliefs [10] which offers a possibility of both studying in detail the growth process and obtaining precise quantitative information on boundary profiles. As it has been mentioned in [2], continuous approach, in contrast to the discrete and dynamic methods, provides a possibility of calculating the relief evolution over large temporal, ~10^3 s, and spatial, ~10^2 μm, scales and allows one to study directly how the source noise and various nonlinear and geometric effects influence the growth process.

The goal pursued by present study includes theoretical investigations of the evolution of the profile boundary statistics during growth due to inhomogeneity of a deposition source and impact of the statistical parameters (i.e. rms roughness, correlation length and Hurst exponent) on the short-wave scattering intensity of Al/Zr multilayer mirrors.

2. Kinetic model and simulation of the growth of multilayer mirrors

2.1 Kinetic model of the rough multilayer growth employed in short-wave optics

In the continuum approach evolution of the multilayer film profile (boundary) height h with time t at point r on the surface is described by a kinetic equation taking into account two processes to wit, deposition and relaxation. Deposition of the material on the film upper boundary increases film profile height reckoned from the initial level h_0, while relaxation smoothes asperities on the film surface [10].

For the sake of simplicity we assume that main relaxation mechanisms during multilayer film growth are surface diffusion and evaporation-condensation [10, 11]. This simplification is acceptable since bulk diffusion is much slower than surface diffusion at the typical growth temperatures and therefore could be neglected.

As for the gratings and mirrors growth [2, 12] one could assume the surface to be isotropic and two-dimensional, in other words, that h can be represented by a function of coordinate x and time t and therefore the rate of height variation $\partial h(x,t)/\partial t$ can be written in the form:

$$\partial h/\partial t = g(x,t) + \nu_2\sqrt{1+\left[\nabla h(x,t)\right]^2}\,K(x) - \nu_4\sqrt{1+\left[\nabla h(x,t)\right]^2}\left[\partial^2 K(x)/\partial x^2\right] \quad (1)$$

where $g(x,t)$ is the flux of atoms onto the film surface, υ_2 and υ_4 are parameters defining the rates of the evaporation/condensation and the diffusion processes, respectively, $K(x)$ is the local curvature of the surface. The three-dimensional function $h(x,y,t)$ can be treated by the same manner and would be discussed elsewhere. Equation (1) describes growth of the thin film in the case of arbitrary height gradients $\nabla h(x,t)$ [10, 11].

The first term in Eq. (1) describes increase of the film height due to deposition of the material, second and third terms determine the smoothening due to evaporation/condensation and diffusion, respectively. Deposition flux $g(x,t)$ is inhomogeneous in space x and time t and it's actual form depends on the type of the source, growth method and conditions of the deposition (e.g. temperature of the substrate):

$$g(x,t) = g_0 + \Delta g(x,t), \quad \langle g(x,t)\rangle = g_0 \quad (2)$$

We note that if $h(x,t)$ varies only weakly with x (the small angle approximation), in other words, $\nabla h(x,t) \ll 1$, Eq. (1) allows simplification. Since $K(x)$ can be written as,

$$K(x) = \frac{\nabla^2 h(x,t)}{\left(1+\nabla h(x,t)\right)^{3/2}} \approx \nabla^2 h(x,t). \quad (3)$$

Equation (1) can be rewritten in the small angle approximation as

$$\partial h/\partial t = g(x,t) + \nu_2\nabla^2 h(x,t) - \nu_4\nabla^4 h(x,t). \quad (4)$$

#232880 - $15.00 USD Received 20 Jan 2015; revised 20 Mar 2015; accepted 22 Mar 2015; published 16 Apr 2015

Equation (4) or similar to it is often used to describe boundary profile evolution of the multilayer mirrors during growth [13–15]. However, Eq. (1) should be applied in simulation of the growth of multilayer mirrors, because here quite frequently $\nabla h(x,t) \sim 1$; as an example may serve, for instance, the case of a significant root-mean square (rms) roughness σ and small surface-roughness correlation lengths ξ. Hence with Eq. (1) one can obtain more accurate results.

2.2 Analysis of the film border profile statistics

In the concluding stage of a study of the growth process one has to define the topology of a grown film. This means that the numerical data obtained for boundary profiles in the course of film growth simulation have to be analyzed to locate quantities which characterize statistically the surface relief. By calculating the dependences of these quantities on the thickness or deposition time of the film, one will be capable of drawing conclusions concerning the process of its growth.

We analyze the variation of roughness of the film (for instance, of the multilayer mirror) by the power spectral density (PSD) function $S(f_x,t)$ with a spatial frequency f_x; then σ is calculated through $S(f_x,t)$. The correlation length is determined from a fitting of the analytical PSD function $S_{An}(f_x,t)$ obtained within a certain correlation model to $S(f_x,t)$ derived from the calculation of $h(x,t)$. Calculated PSD functions can be decomposed within the different correlation models: auto-regressive moving average model (ARMA) [16], time-invariant linear filter model (TILF) [17], ABC or K-correlation model [18], Shifted-Gaussian model [19] and Fractal model [20]. Three correlation models are used in this study to decompose PSD functions calculated numerically: the ABC model, the Shifted-Gaussian model and the Fractal model.

The ABC model sufficiently accurately describes surface roughness over large length scales. The PSD function and correlation length ξ_{ABC} in the ABC model are given by [18],

$$S_{ABC}(f_x) = \frac{A}{\left[1+\left(Bf_x\right)^2\right]^{(C+1)/2}}, \quad \xi_{ABC} = \frac{(C-1)^2 B^2}{2\pi^2 C}, \tag{5}$$

where A, B, C are fitting parameters.

The Shifted-Gaussian PSD function is used to characterize a contribution to the surface roughness from a surface superstructutre and has the following form [19]:

$$S_{SG}(f_x) = \pi^{3/2}\sigma^2\xi_{SG}\left\{\exp\left[-\xi^2\left(f_x - f_{SG}\right)^2/4\right] + \exp\left[-\xi^2\left(f_x + f_{SG}\right)^2/4\right]\right\} \tag{6}$$

In Eq. (6) σ, ξ_{SG} and f_{SG} correspond to the rms roughness, correlation length (i.e. size of the superstructure) and periodicity of the superstructure, respectively.

The Fractal model is applied in order to describe self-affine surface topography. In this model PSD is represented by the power law function [20]:

$$S_{Fr}(f_x) = \frac{P}{f_x^n}. \tag{7}$$

Here P and n are the spectral strength and spectral index, respectively. The correlation length ξ_{Fr} in the Fractal model is given by

$$\xi_{Fr} = \frac{(n-1)^2 L}{2(2n-1)}, \tag{8}$$

where L is the substrate length.

In the present study the analytical PSD function has been calculated as the sum of three PSD functions:

#232880 - $15.00 USD Received 20 Jan 2015; revised 20 Mar 2015; accepted 22 Mar 2015; published 16 Apr 2015

$$S_{An}(f_x) = S_{ABC}(f_x) + S_{SG}(f_x) + S_{Fr}(f_x). \quad (9)$$

We assume that the initial height distribution probability density is described by the Gaussian function and that the autocorrelation function (AF) $C(x)$ is an exponent

$$C(x) = \sigma^2 \exp\left\{-\frac{x^{2D}}{\xi^{2D}}\right\}, \quad (10)$$

where $0 < D \leq 1$ is the Hurst exponent (scaling roughness parameter). For $D = 1$, the function $C(x)$ represents the Gaussian AF, for $D = 0.5$ – the Exponential AF. The topology of boundaries obtained by simulation of the growth process can be analysed by a variety of statistical parameters and of methods of their calculation.

2.3 Simulation of the growth of multilayer Al/Zr mirrors

Consider the effect of source noise produced on surface roughness of a multilayer Al/Zr mirror. Equation (1) without the second term corresponding to the condensation/evaporation smoothing has been used to describe the evolution of the profile shape. The second term in Eq. (1) can be eliminated from the consideration since its influence on the surface roughness is rather small in the case of the Al/Zr mirror growth [12, 15]. However, there are other issues expect source noise affecting roughness, such as intermixing at the Al/Zr boundary and amorphous-to-crystalline transitions in Al layers [21].

The parameters of the Al/Zr mirror under study were chosen as follows: the period of the multilayer structure $\Delta = 10.45$ nm, the ratio of the Zr layer thickness to Δ, $\Gamma = 0.4$, the mirror length $L = 10$ μm, $\sigma(t = 0) = 0.084$ nm, $\xi(t = 0) = 10$ nm [22]. The source noise parameters, i.e. the fluctuation amplitude Δg, the spatial length of deposition nonuniformity l_g and the time of existence of the nonuniform noise t_g, have been varied within 0.1–0.3 g_0, 1–100 nm and 10^{-3}–10^{-1} sec intervals, respectively. Values of $g_0 = 0.5$ nm/s and parameters υ_4(Al) = 125 nm^3/s, υ_4(Zr) = 100 nm^3/s have been taken from the previous study [2, 12].

To calculate values of the deposition noise $\Delta g(x,t)$ the following algorithm is used. First, a substrate, i.e. a mirror, divides on segments with the random length l_r less then a value of the spatial length of the deposition nonuniformity l_g. Then, for each segment a random value Δg_r of the fluctuation amplitude ($-\Delta g < \Delta g_r < \Delta g$) generates. Values of the l_r and Δg_r are recalculated after t_g time. For the sake of simplicity of the consideration we introduce the parameter $q = \Delta g t_g$ (measured in nanometers) which characterizes the amount of the deposited material due to imperfection of the deposition source. Calculations of σ through $S(f_x,t)$ have been averaged over eight realizations. To simulate growth of the Al/Zr mirror Eq. (1) was solved numerically with the help of the finite difference method under periodic boundary conditions.

Figure 1 displays the results of the calculations of σ obtained for different source noise parameters q and l_g, vs. the total multilayer thickness H.

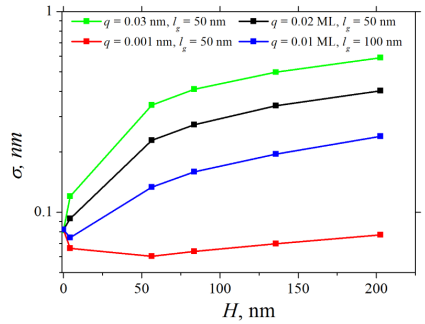

Fig. 1. Rms roughness σ of the Al/Zr mirror obtained for different source noise parameters q and l_g vs. total multilayer thickness H.

#232880 - $15.00 USD Received 20 Jan 2015; revised 20 Mar 2015; accepted 22 Mar 2015; published 16 Apr 2015

As follows from the examination of Fig. 1 the evolution of σ is strongly dependent on values of q. As in the previous study [12] the film roughness at the initial stage of growth decreases due to smoothening of the roughness associated with the substrate. Wherein the greater is values of q the shorter is the period during which the initial roughness affects on the growth process.

Plotted in Fig. 2 are σ vs. H variations in time calculated for equal values of q = 0.01 nm and different values of l_g. The data were obtained for the same set of deposition and relaxation parameters. As follows from Fig. 2 the film roughness for l_g = 100 nm increases faster than for l_g = 50 nm. Such dependence of the surface roughness on the deposition flux spatial nonuniformity is analogous to the influence of the initial correlation length ξ_0 of roughness on film profile variations [12]. This behavior is caused by the stronger smoothing of relief asperities with a larger local surface curvature $K(x,t)$. For l_g = 100 nm spatial sizes of asperities are higher than for l_g = 50 nm while asperities heights are the same. Therefore, local surface curvature $K(x,t)$ is higher for l_g = 50 nm than for l_g = 100 nm which results in a stronger smoothening of the surface roughness and give smaller values of σ.

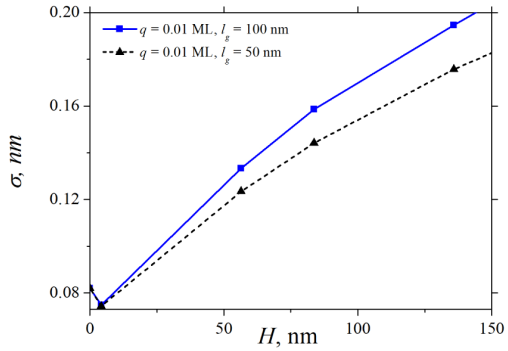

Fig. 2. σ vs. H variations of the Al/Zr mirror obtained for different source noise parameters l_g.

In Fig. 3 calculated PSD functions at different boundaries in Al/Zr structure are shown. Calculations of the Al/Zr structure growth were performed for the following source noise parameters: q = 0.03 nm, l_g = 50 nm. From Fig. 3 is clearly seen that rms roughness increases during growth process and the shapes of three curves are similar. The shape of the PSD function curve depends on the source noise parameters significantly.

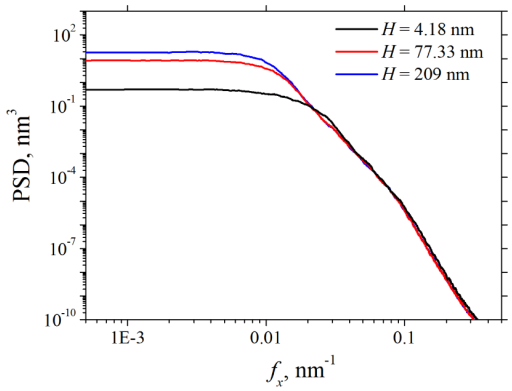

Fig. 3. Calculated PSD functions on boundaries of the Al/Zr multilayer structure of different thickness H.

Changes in the source noise parameters may lead to changes in the shape of the PSD function curve, as seen in Fig. 4. Figure 4 displays the calculated PSD function obtained with following source noise parameters: q = 0.01 nm, l_g = 1 nm. In Fig. 4 the analytical PSD

#232880 - $15.00 USD Received 20 Jan 2015; revised 20 Mar 2015; accepted 22 Mar 2015; published 16 Apr 2015

function also is shown as the sum of three PSD functions obtained with different correlation models. Calculations of the profile evolution were performed for the following source noise parameters: q = 0.01 nm, l_g = 1 nm. From the fitting of $S_{An}(f_x,t)$ to $S(f_x,t)$ the parameters for each of three PSD functions have been found. The correlation lengths of the surface roughness obtained from those parameters were estimated: ξ_{ABC} = 93.3 nm, ξ_{SG} = 160 nm, ξ_{Fr} = 781 nm.

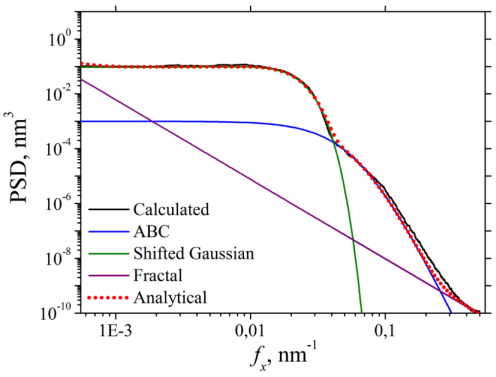

Fig. 4. Calculated and analytical PSD functions of an Al/Zr mirror. Combined PSD function is obtained as a sum of three analytical PSD functions: ABC, Shifted Gaussian and Fractal.

Boundary profiles obtained with the kinetic model accounting different relaxation mechanisms and the source noise could be used as initial data for the calculation of scattering intensities.

3. Rigorous calculus of soft x-ray and EUV scattering intensities of rough mirrors

Despite the significant progress reached in development of exact numerical methods for the study of wave diffraction by random boundary roughness [23], only asymptotic and approximate approaches were available until quite recently for the investigation of x-ray and cold neutron beam scattering intensities, such as the Kirchhoff scalar integral approximation, the Born approximation, the distorted-wave Born approximation, the parabolic wave equation method, the Rayleigh method and a few others [3, 8]. Drawing from the mentioned above MIM, we are passing on now to a study of the effect of boundary topology in a continuum film on short-wave scattering intensity. The MIM identified that the intensities of x-ray scattering at boundaries with random roughnesses may differ considerably (by a few times) from the values derived with the use of various approximate models [8]. It was also found that this method operates equally well with asperities of any kind and shape which obey arbitrary statistics of distribution: periodic, quasi-periodic, random Gaussian or non-Gaussian, any their combinations and, more importantly, real (measured or simulated) [8, 9, 12, 24].

3.1 EUV scattering intensity using profiles of Al/Zr grown model boundaries

We study numerically EUV mirrors having 20 pairs of Al/Zr layers deposited by magnetron sputtering with Γ_{Zr} = 0.4, Δ = 10.45 nm and H = 209 nm [15, 22]. In the present work the boundary profiles were grown by the described above growth model using the substrate roughness with σ_0 = 0.084 nm and ξ_0 = 10 nm. As it has been demonstrated [12], the initial (substrate) correlation length ξ_0 has no influence on the almost all grown boundary profiles (except, may be, a few first) and the initial rms roughness σ_0 has minor influence (in the range of small values σ_0) on those boundary profiles. Hence, the scattering intensities of the multilayer can be calculated with any set of substrate parameters in the range. The typical one-dimensional AFM scans of the substrate and also of the upper boundary measured in the space range of 1 μm can be found in [15]. The calculations of the profile evolution were performed for the following set of parameters: deposition rate g_0 = 0.5 nm/s, Δg = 0.3 nm/s,

#232880 - $15.00 USD Received 20 Jan 2015; revised 20 Mar 2015; accepted 22 Mar 2015; published 16 Apr 2015

v_4(Al) = 125 nm^3/s, and v_4(Zr) = 100 nm^3/s. It is worth note that both experimental and theoretical grown parameters of mirrors (witnesses) were similar to those as for the EUV grating producing with the same multilayer coating on the etched Si substrate [12, 22].

Figures 5 and 6 display the multilayer mirror spectral reflectances $\eta(\lambda)$, which were averaged by Monte Carlo and calculated for two incident angles $\theta = 5°$ and $\theta = 30°$. Several boundary profile realizations are enough to rich the statistical convergence due to important role of the noise of a source in the growth process and purely random nature of the high-frequency roughness part of each boundary. The respective measured curves can be seen in Figs. 3 and 4 of Ref [22] and they agree with the calculated data with the plot accuracy. The approximated models accounting or non-accounting (perfect layers) such roughness type on vertically non-correlated boundaries by well-known Debye-Waller amplitude factors applied on each boundary together with the recursive Parratt relations have been also used to compare with the exact model. However, in these approximations one cannot use the lateral correlation length parameter and do not know exactly how the rms roughness changes from the substrate to the upper boundary of the multilayer mirror. Thus, in such and even more sophisticated approximations [13–15] only average or scaled rms roughness and correlation length parameters can be used together with an approximated model of scattering intensities. In our model, appropriate and direct material growth and noise parameters of the particular technology have been used and, thus, realistic (close to measured ones) boundary profiles were obtained and applied. Besides, we do not use in the scattering intensity model any approximations, except those required for the numerical implementation of the Maxwell solver and Monte Carlo simulation. A rigorous approach employed to take into account the contribution due to random roughness incorporated in the growth model brings about a decrease in the specular scattering intensity and a redistribution in the diffuse scattering intensity, which have been determined by means of PCGrate® in the approach described in this section. The refraction indices for Al were taken from Ref [26], and those for Zr, from Ref [25], because of the absence of the relevant data for Zr in [26]. As established earlier [27–29], in the wavelength range of interest, 17–22 nm, the refraction indices of some materials derived from the approach developed in [25] may be not accurate enough.

A comparison of calculated with measured specular reflection coefficients of the multilayer mirror revealed that boundary profile parameters obtained from the growth model of the multilayer Al/Zr mirror correlate well with the real boundary profile values. Like this, the upper interface roughness of $\sigma_H \approx 0.4$ nm derived from the growth model is close to the measured value of $\sigma \approx 0.3$ nm taking into account that the calculated data have been derived from the space range of 10 μm and the measured data – from 1 μm [15]. The middle frequency component of surface roughnesses increases by an order of the magnitude as compared to the Si substrate. The knee in the white noise roughening is apparent on the measured PSD curve at a frequency of ~0.01 nm. The calculated correlation length value of $\xi_H \approx 103.5$ nm derived from the K-correlation model agrees very well with that measured value. Besides, the data obtained in this comparison argue for a ~90% of the TE polarized incident radiation (intensity).

As one can see in Fig. 5, the best fitted (to measured data and also to rigorous calculus) approximation using the same Debye-Waller factor for all boundaries gives a good coincidence in the scattering intensity maxima for $\theta = 5°$. However, the maxima position in the approximated curve little bit shifted to the left and it is narrower in respect to the exact curve, so that the right slope values in this curve differ valuably (more than 10%) from the respective exact values.

#232880 - $15.00 USD Received 20 Jan 2015; revised 20 Mar 2015; accepted 22 Mar 2015; published 16 Apr 2015

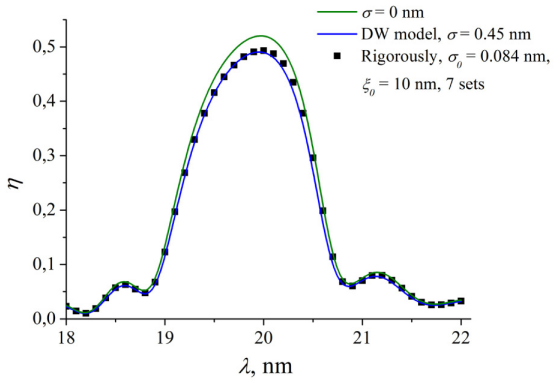

Fig. 5. Spectral reflectances of Al/Zr multilayer mirrors, which were calculated for an incident angle $\theta = 5°$ using: perfect boundaries (green line); the rigorous approach averaged over seven grown model realizations (points); Debye-Waller amplitude factors with rms roughness of 0.45 nm (blue line).

The same approximation model applied to the case of $\theta = 30°$ (see Fig. 6) gives substantial differences even in the maxima. The slope values for $\theta = 30°$ in the approximated curve can differ from the exact values more than 20%. Thus, in addition to rather big differences in specular scattering intensity values, the approximated model gives for both incident angles an overestimated (averaged) value of the rms roughness ($\sigma = 0.45$ nm) even for the last (upper) boundary. Of course, this value is far from realistic one for first boundaries for which σ should be close to $\sigma_0 = 0.084$ nm. For the calculations discussed above, good convergence of results is observed and $N = 1000$ per boundary is required to simulate the quantity η of the mirror having piecewise linear boundaries with an error of no worse than $\sim 10^{-4}$ which is estimated from the energy balance.

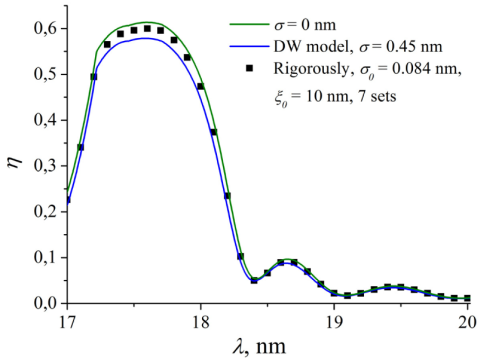

Fig. 6. The same as in Fig. 5, but for $\theta = 30°$.

The dependence between the rigorously calculated diffuse scattering intensity vs. the angle of scattering is presented in Fig. 7. The average curve was determined at a wavelength $\lambda = 20$ nm and the 90% TE-polarized radiation via the Monte Carlo method using statistical realizations. The same seven sets of 41 grown boundary profiles (including substrates) as for the specular light intensity calculation and $N = 1200$ have been used to achieve the better accuracy of the results. The accuracy derived from the energy balance criterion is $\sim 10^{-5}$. The diffuse scattering intensity level near the specular peak is $\sim 10^{-4}$ that is small enough for such a multilayer. The main shape of the diffuse scattering intensity is close to Gaussian.

#232880 - $15.00 USD Received 20 Jan 2015; revised 20 Mar 2015; accepted 22 Mar 2015; published 16 Apr 2015

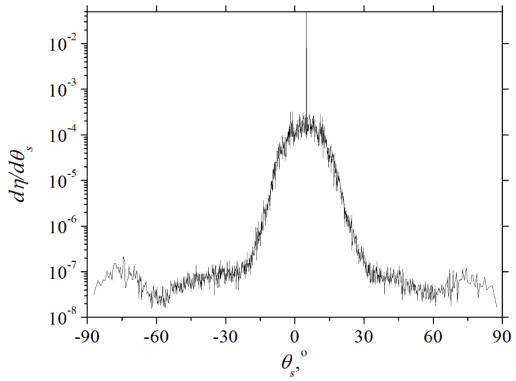

Fig. 7. Scattering intensity of the Al/Zr mirror which was calculated rigorously by averaging over seven grown model realizations for an incident angle $\theta = 5°$ and $\lambda = 20$ nm vs. angle of scattered radiation θ_s.

4. Conclusion

In the present study we proposed the complex approach to the boundary profile determination and short-wave scattering intensity analysis. The approach includes simulation of the multilayer film growth and computation of soft-x-ray–EUV scattering intensities from the growth-model-obtained boundary profiles.

We investigated the influence of the source noise parameters and initial boundary profile parameters on the evolution of the Al/Zr layer reliefs. It was obtained that amount of the material q deposited due to imperfection of the deposition source affects most strongly the rms roughness of boundary profiles. Statistical analysis has demonstrated that the surface topography evolves into the complex structure during the growth process and represents the composition of different topographies. The shape of the PSD function depends significantly not only on the substrate roughness, relaxation mechanism and on the source noise parameters as well. The study of Al/Zr mirrors demonstrates for the first time that the boundary growth of multilayer mirrors with a large height and jumps of the profile gradient can be correctly simulated by precisely allowing for the local curvature of the surface and accounting the inhomogeneity of material deposition on the substrate. Diffuse (intermixing) boundaries can be also treated in the continuum growth model that should be addressed to the future publication.

The complex mirror model taking exactly into account effects of growth kinetics of boundaries having random roughnesses with varying rms and correlation lengths demonstrates very good correlation of specular reflectance values with the data obtained on the synchrotron radiation (SR) source for a number of incidence angles and wavelengths. The discrepancy between values of the measured reflectance and those obtained in our simulation is in the range of plotting accuracy. As for the calculations discussed here, their results exhibit good convergence and accuracy, with N = 1000–1200 required for simulation of η of multilayer mirrors with polygonal, randomly-rough boundaries, with an error ~0.01–0.001% evaluated from the energy balance consideration.

Owing to efficient algorithms and the potential of the developed vector electromagnetic PCGrate code, a standard PC can be employed to examine multilayer mirrors with any kind of roughnesses. The investigations are carried out with the help of data obtained by the simulation of the boundary profile growth and provide theoretical results making it possible to predict the intensities of soft-x-ray–EUV scattering of multilayer mirrors with an accuracy equivalent to that of measurements based on SR sources. The proposed numerical simulation permits one to radically cut the cost of technological processes and measurements on multilayer mirrors with a desired boundary surface structure, an approach aimed at reaching

#232880 - $15.00 USD Received 20 Jan 2015; revised 20 Mar 2015; accepted 22 Mar 2015; published 16 Apr 2015

values of the specular reflectance close to the theoretical limit and, at the same time, lowest levels of diffuse scattering near specular peaks.

The model describing growth of multilayer films can be successfully used, in its turn, in studies of the growth process in semiconductor structures, more specifically, super-lattices, distributed Bragg reflectors, multiple low-dimensional nanocrystals, etc. The boundary integral equation method developed for analysis of the intensity of short-wave scattering by multilayer randomly-rough mirrors with any roughness statistics can also be applied with considerable efficiency in studies of various surfaces designed to operate in other spectral ranges, photonic crystals, Fresnel zone plates and spectral diffraction gratings of any kind.

Acknowledgments

This work was partially supported by Russian Foundation for Basic Research (grant 14-02-00391-a).

#232880 - $15.00 USD Received 20 Jan 2015; revised 20 Mar 2015; accepted 22 Mar 2015; published 16 Apr 2015